ALCHERINGA: AN AUSTRALASIAN JOURNAL OF PALAEONTOLOGY
https://doi.org/10.1080/03115518.2026.2697810

Investigation of finger motion in two quadrupedal dinosaurs: the sauropod *Camarasaurus* and stegosaur *Stegosaurus*

Philip J. Senter

ABSTRACT

The metacarpals of sauropod dinosaurs were arranged to form a tube or semi-tube, and those of stegosaurs were arranged to form a semi-tube. This orientation aimed the fingers toward each other during flexion and would have caused the fingers to crowd each other and obstruct each other's movements during flexion if the fingers were as mobile as they were in other dinosaurs. I therefore sought to determine whether finger movement in members of these two lineages involved any special modifications to prevent such obstruction. I posed the bones of the hand skeletons of the sauropod *Camarasaurus* sp. and the stegosaur *Stegosaurus sulcatus* in sandboxes to measure their range of motion (ROM). The results indicate that limitations upon finger mobility in both *Camarasaurus* and *Stegosaurus* prevented the fingers from crowding each other or obstructing each other's movement. In *Camarasaurus*, ROM in fingers I–IV was limited to the field of hyperextension. In *Stegosaurus*, ROM in finger II was limited to the field of hyperextension, and the other fingers were immobile. These two dinosaur lineages thus provide a remarkable example of convergent evolution, not only in metacarpal configuration but also in the special modification (limited finger mobility) to prevent the potential predicament (fingers obstructing each other's movements) that said configuration would otherwise have caused.

ARTICLE HISTORY
Received 29 April 2026
Revised 23 June 2026
Accepted 29 June 2026

KEYWORDS
Dinosauria; Sauropoda; Stegosauria; manus; functional morphology; range of motion

Philip J. Senter [psenter@uncfsu.edu], Department of Biological and Forensic Sciences, Fayetteville State University, 1200 Murchison Road, Fayetteville, North Carolina 28301, USA.

RANGE OF MOTION (ROM) within the hand has previously been investigated in numerous species of bipedal dinosaurs, including theropods (Osmólska & Roniewicz 1969, Galton 1971, Welles 1984, Nicholls & Russell 1985, Sereno 1994, Gishlick 2001, Carpenter 2002, Kobayashi & Barsbold 2005, Senter 2005, 2006a, 2006b, Senter & Parrish 2005, Senter & Robins 2005, Senter & Sullivan 2019, Kobayashi *et al.* 2025) and a basal sauropodomorph (Mallison 2010; Reiss & Mallison 2014). ROM within the hand has been investigated previously in only two species of quadrupedal dinosaurs: the ceratopsian *Leptoceratops gracilis* Brown, 1914 (Senter 2007) and the iguanodontian ornithopod *Uteodon aphanoecetes* (Carpenter & Wilson, 2008). Limb proportions and forelimb configuration in *L. gracilis* suggest an ability to alternate between bipedal and quadrupedal modes of locomotion (Coombs 1978), whereas in *U. aphanoecetes* the limb proportions and forelimb configuration are more consistent with primarily quadrupedal locomotion (Carpenter & Wilson 2008). Here, I present a study of ROM within the hands of two more quadrupedal dinosaurs: *Camarasaurus* Cope, 1877 and *Stegosaurus sulcatus* Marsh, 1887. *Camarasaurus* is a genus of sauropod dinosaur from the family Camarasauridae (Upchurch *et al.* 2004). *Stegosaurus* Marsh, 1877 is a genus of stegosaur from the family Stegosauridae (Galton & Upchurch 2004). Both are from the Morrison Formation (Upper Jurassic) of western North America (Galton & Upchurch 2004, Upchurch *et al.* 2004).

Previous studies have determined that the metacarpals of sauropods, stegosaurs, and ankylosaurs were arranged in a tight arc in proximal view, with their long axes parallel to each other, so that the metacarpus formed a tube or a semi-tube (Hatcher 1902, Janensch 1961, Bonnan 2003, Apesteguía 2005, Carpenter *et al.* 2008, Senter 2010, 2011, Tschopp *et al.* 2015). This is unusual among tetrapods, and it prompts important questions, such as the following. How does ROM within the hand differ in these dinosaurs from ROM within the hands of quadrupedal dinosaurs without a tubular or semi-tubular metacarpus? Since a tubular or semi-tubular metacarpal configuration aims the fingers toward each other during flexion, how did the fingers avoid crowding each

Published online 27 Jul 2026

other or obstructing each other's movement during flexion in dinosaurs with such metacarpal configurations? I undertook this study to answer these questions.

Several recent studies have shed light on the influence of soft tissues on ROM in the limbs of archosaurs and other reptiles (Holliday *et al.* 2010, Hutson & Hutson 2012, 2013, Arnold *et al.* 2014, Kambic *et al.* 2017, Manafzadeh & Padian 2018, Senter & Sullivan 2019, Demuth *et al.* 2023). The results of such studies indicate that soft tissues have a major influence upon ROM at proximal limb joints such as the hip, shoulder, and elbow. Measurements of ROM in these joints, as found with bare bones (using the assumption that the edges of bony articular surfaces indicate the limits of ROM), differ from ROM at these joints in the intact animal, often by a large percentage (Hutson & Hutson 2012, 2013, Arnold *et al.* 2014, Manafzadeh & Padian 2018, Senter & Sullivan 2019). However, the same is not the case for joints within the hand. The metacarpals and phalanges of the hands of most dinosaur species articulate tightly with each other and maintain tight articulation through the arc of motion, which suggests that the influence of intervening soft tissues on ROM is minimal. This inference is supported by experiments with alligator metacarpals and phalanges. Those experiments showed that ROM within the hand, as found with bare bones, differs little from ROM as found in the intact animal (Hutson & Hutson 2015). Hutson & Hutson (2015) concluded that phalangeal ROM is greater with bare bones than in the intact animal, but their fig. 3 shows that this difference is small and that there is broad overlap between the two. This suggests that in studies of extinct archosaurs, it is realistic to use bare-bones ROM to approximate ROM within the hand of the living animal, with the caveat that phalangeal ROM may have been slightly less in the living animal than that found with bare bones.

Materials and methods

To determine the maximum amount of extension and flexion at each joint, I assumed that the edges of the articular surfaces delineated the limits of motion, as in previous studies of dinosaur manual ROM (see references listed above). I used the following protocol to measure the two-dimensional ROM of each finger within the plane of finger motion. I posed the metacarpal and phalanges of the finger in articulation in a sandbox, pollucal side up, and photographed each finger in full hyperextension and full flexion, from above. To minimize parallax between the hyperextension photo and the flexion photo, I kept the metacarpal immobile and moved only the phalanges, and I snapped both photographs from the same position in space by keeping the camera screwed onto the arm of an overhead camera mount, with the viewfinder centred on a locus near the distal end of the metacarpal that approximated the centre of rotation of the proximal phalanx. I digitally superimposed the photos, drew a line down the proximodistal axis of each phalanx, and measured ROM at each joint as the angle between the lines (Figs 1 and 2). I used Microsoft Paint 11.2507.371.0 (Microsoft Corporation 2025) for the digital superimposition, Microsoft PowerPoint 2605 (Microsoft Corporation 2026) for the drawing of the lines, and a transparent protractor held by hand against a computer screen for the measuring of the angles. I defined the proximodistal axis of each non-ungual phalanx as a line running through the centres of the proximal and distal surfaces of the phalanx in the view of the plane of flexion and extension (the plane in which the photos were taken in Figs 1A, B, E–G, I, J and 2). I defined the proximodistal axis of each ungual phalanx as a line perpendicular to a line connecting the proximal surfaces of the dorsal and palmar lips of the phalanx in the view of the plane of flexion and extension. I used this protocol on the left and right hands of American Museum of Natural History (AMNH), New York, USA. FARB 823 (*Camarasaurus* sp.) and the right hand of National Museum of Natural History, Smithsonian Institution (formerly United States National Museum [USNM]), Washington DC, USA. 4937 (*Stegosaurus sulcatus*). I additionally used manual manipulation of the hand bones of three other *Camarasaurus* sp. to compare with the results from AMNH FARB 823. The other three *Camarasaurus* sp. specimens are AMNH FARB 332 (which includes a partial right hand with metacarpals I–V and the proximal phalanx of fingers II–V), 712 (which includes a partial left hand with metacarpals I–V and the proximal phalanx of fingers IV and V) and 965 (which includes a partial right hand with metacarpals I–V, phalanx I-2, and the proximal phalanx of fingers II–V).

I used the following protocol to investigate the three-dimensional motion of the fingers of *Camarasaurus* sp. (AMNH FARB 823: right and left hands) and *S. sulcatus* (USNM 4937: right hand). I posed the metacarpals in articulation, distal end down, in a sandbox. I then posed the phalanges in articulation with the metacarpus, to recreate the configuration of the hand skeleton of the standing animal

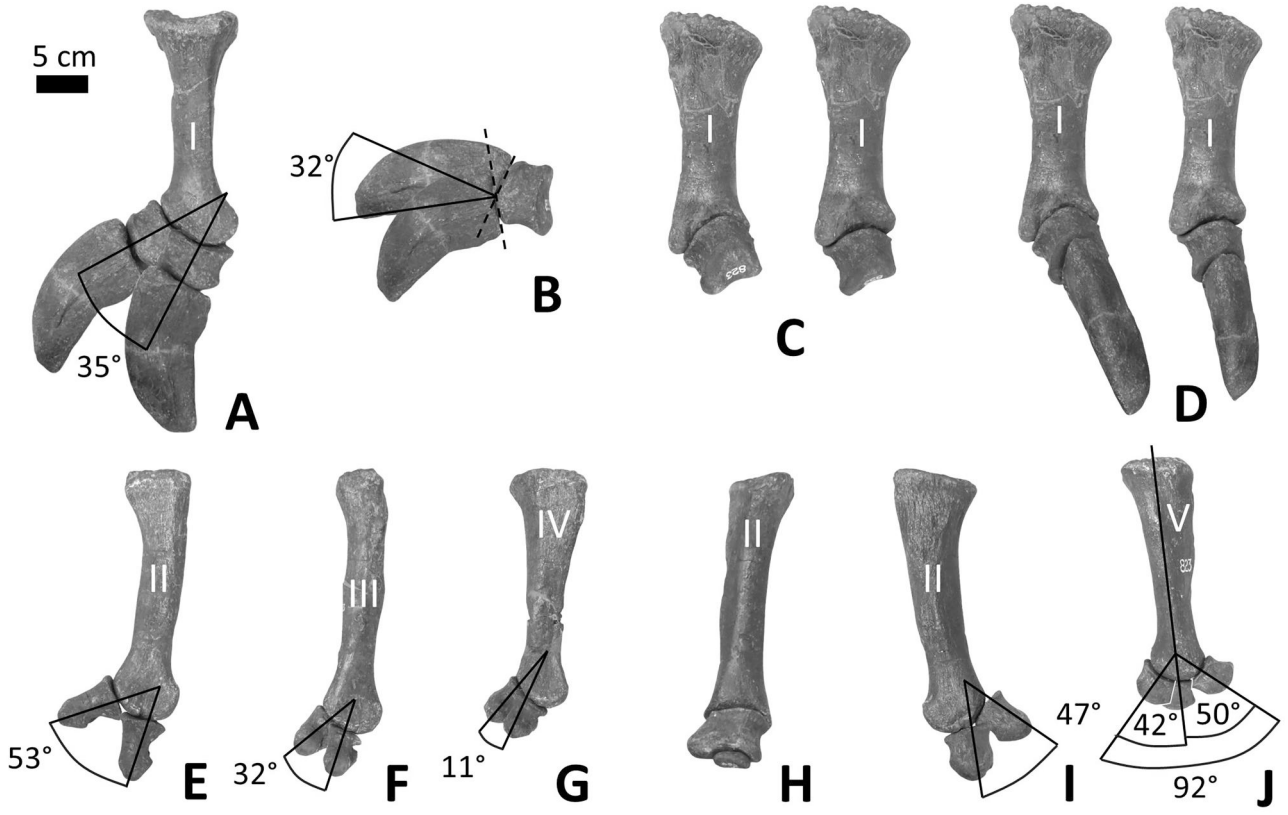

Fig. 1. Range of motion (ROM) in the fingers of *Camarasaurus* sp., AMNH FARB 823. **A**, ROM of phalanx I-1 of the right hand. **B**, ROM of phalanx I-2 (thumb ungual) of the right hand. **C**, View toward extensor surface of metacarpal I, showing torsion in the position of phalanx I-1 as it moves from full hyperextension (left image) to full flexion (right image). **D**, Same as sub-figure C, with phalanx I-2 added. **E**, ROM of phalanx II-1 of the right hand. **F**, ROM of phalanx III-1 of the right hand. **G**, ROM of phalanx IV-1 of the right hand. **H**, View toward extensor surface of metacarpal II of the left hand, showing articulated phalanges II-1 and II-2. **I**, ROM of phalanx II-1 of the left hand. **J**, ROM of phalanx V-1 of the left hand. Here and in subsequent figures, I–V = digits I–V.

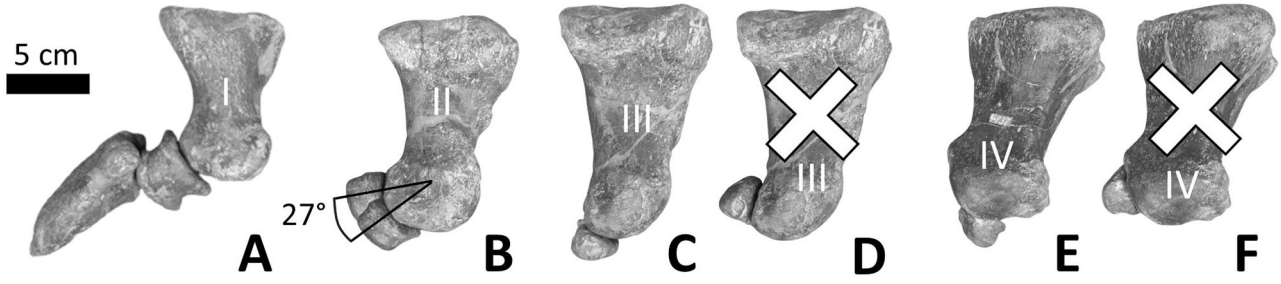

Fig. 2. ROM in the fingers of the right hand of *Stegosaurus sulcatus*, USNM 4937. **A**, Lack of ROM in digit I. **B**, ROM of phalanx II-1. **C**, Lack of ROM of phalanx III-1. **D**, Incorrect pose with phalanx III-1 pressed against a surface on the metacarpal with which the phalanx fits well but which is a non-articular surface and is therefore a location that the phalanx did not occupy in the living animal. **E**, Lack of ROM of phalanx IV-1. **F**, Incorrect pose with phalanx IV-1 pressed against a surface on the metacarpal with which the phalanx fits well but which is a non-articular surface and is therefore a location that the phalanx did not occupy in the living animal.

with its fingers extended and photographed the articulated hand from different angles (Figs 3, 4). For *Camarasaurus*, I then posed the metacarpals in articulation, distal end up, in the sandbox, and posed the phalanges atop them to recreate the configuration of the hand skeleton of the animal with its fingers flexed (Fig. 5). Special precautions were necessary to protect the fossil bones from harm during the posing of the articulated hand skeletons for photography. These included the use of plastic-coated wire twists as non-abrasive fasteners where needed for the articulated metacarpus of *Camarasaurus* (Figs 3 and 5), the use

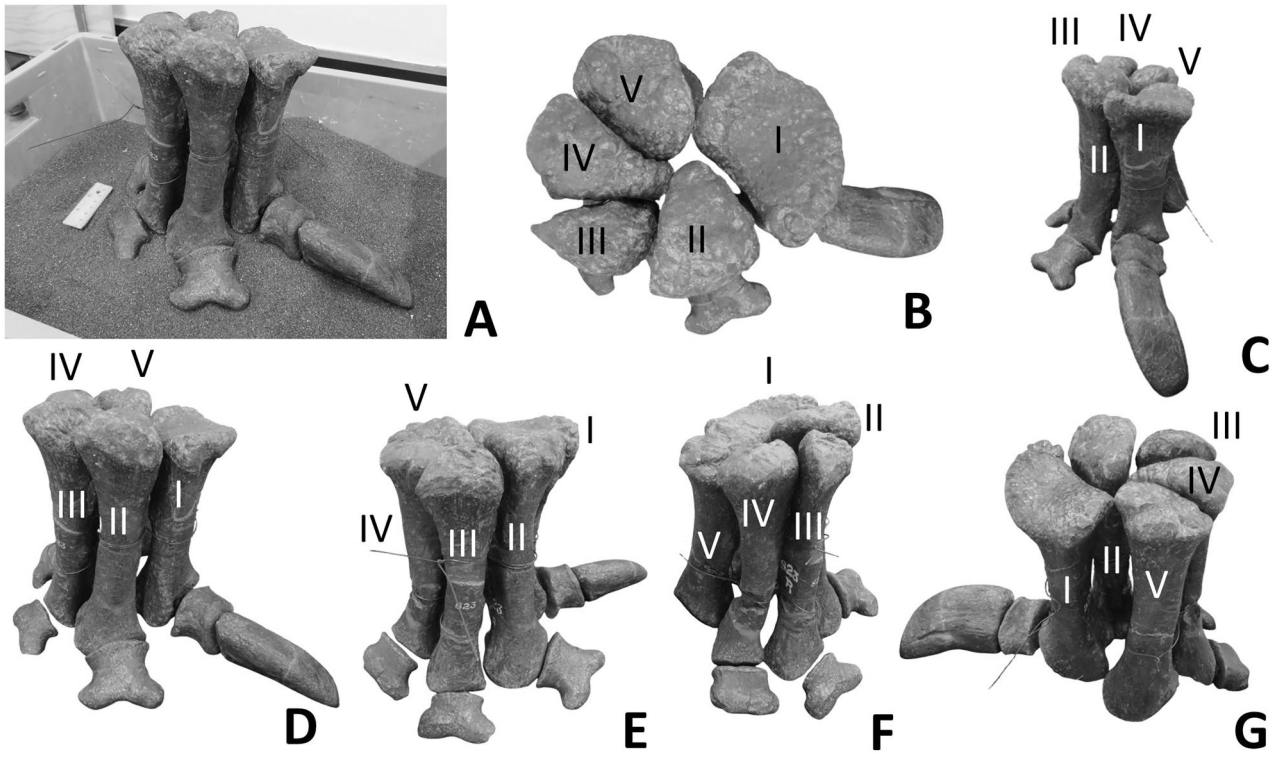

Fig. 3. Articulated right hand skeleton of *Camarasaurus* sp., AMNH FARB 823, posed as if the animal is standing. The sub-figures are reproduced at slightly different scales. Note the ruler in sub-figure A, which shows the size of the articulated hand skeleton. **A**, the articulated specimen in the sandbox used for posing. **B**, Proximal view of articulated hand. **C–G**, Oblique views of articulated hand.

of the horizontal arm of a plastic camera mount to support the thumb ungual of *Camarasaurus* (Fig. 5A), and the use of small polyurethane foam blocks to support the first metacarpal of *Stegosaurus* (Fig. 4).

For this study, I manually manipulated real objects (bones) in real space. Digital techniques are available that enable the digital use of images on a computer screen to perform equivalent or related tasks, and some such techniques have provided useful insights into limb motion in animals (Thompson & Holmes 2007, Mallison 2010, Pierce *et al.* 2012, Baier & Gatesy 2013, Arnold *et al.* 2014, Kambic *et al.* 2014, 2017, White *et al.* 2015, 2016, Manafzadeh & Padian 2018, Demuth *et al.* 2020, 2023, Manafzadeh & Gatesy 2021, Richards *et al.* 2021, Wiseman *et al.* 2022, Dempsey *et al.* 2023, Manafzadeh *et al.* 2024). Digital manipulation of computerized images of scanned forelimb bones on a computer screen (e.g. White *et al.* 2015) produces results similar to those found by manual manipulation of real bones or casts in real space (e.g. Senter 2006a, 2006b, Senter & Parrish 2006). The same is the case for the hindlimb, e.g. White *et al.* (2016) in comparison to Senter (2009). Digital techniques are sometimes necessary to overcome logistical difficulties in the use of real bones or casts. For example, if fossil limb bones remain embedded in matrix, computerized scans of them can be used to measure ROM by digital manipulation (Pierce *et al.* 2012). No such logistical difficulties were present in the study reported here, so digital manipulation was not necessary.

Results

Camarasaurus sp.

The ROM through which the manual phalanges of *Camarasaurus* can move while maintaining tight articulation with their respective metacarpals is very small. Here and below, a phalanx is considered to have lost tight articulation with its metacarpal when a gap appears between the phalanx and the metacarpal. In the right hand of AMNH FARB 823, I found the two-dimensional osteological ROM of the proximal phalanx, in the plane of flexion and extension, to be only 35° in digit I, 53° in digit II, 32° in digit III and 11° in digit IV (Fig. 1A, E–G; Table 1). ROM is similar in the available hand joints of AMNH FARB 332, AMNH FARB 712 and AMNH FARB 965. The proximal phalanx of digit V in the right hand of AMNH FARB 823 is missing.

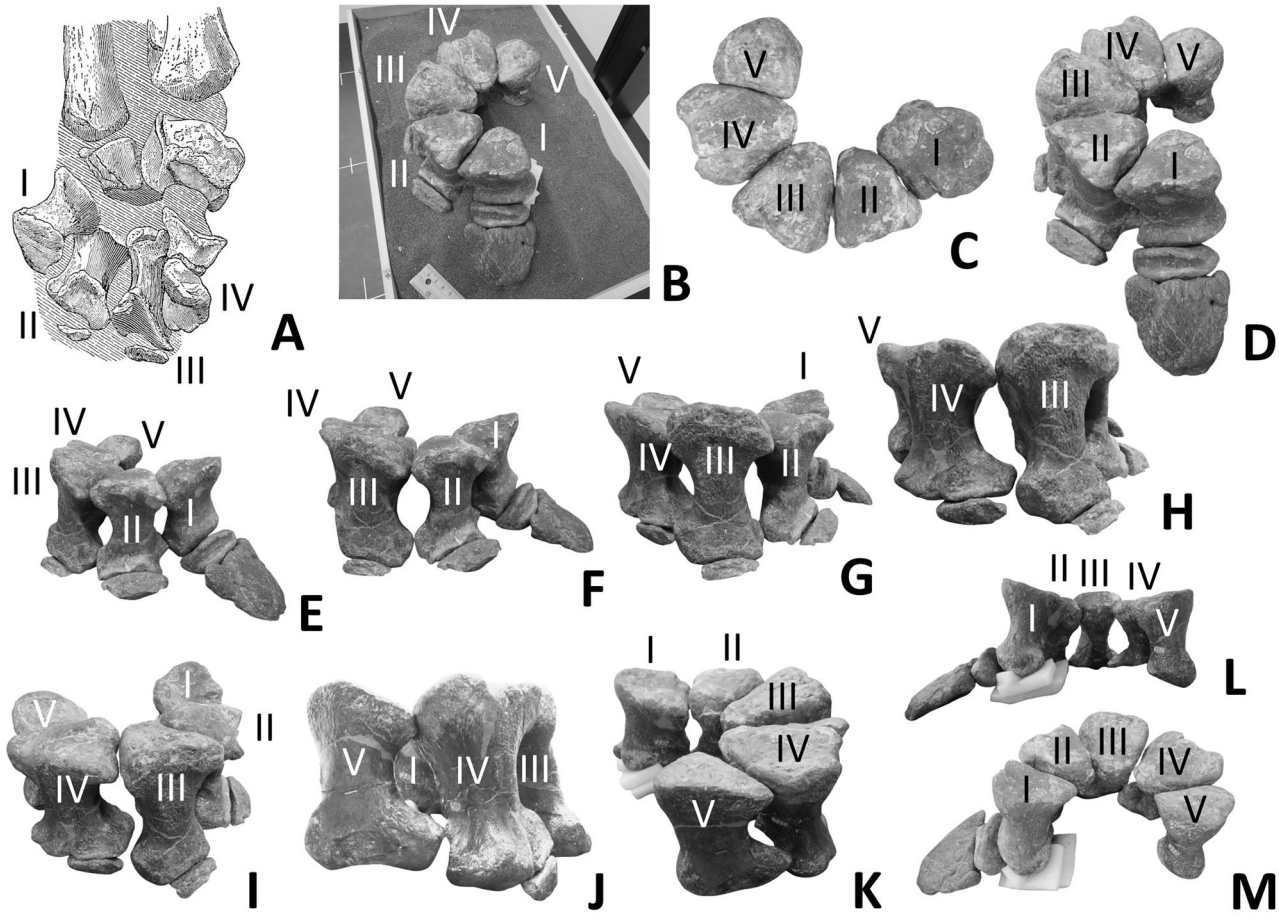

Fig. 4. Articulated right hand skeleton of *Stegosaurus sulcatus*, USNM 4937, posed as if the animal is standing. The sub-figures are reproduced at slightly different scales. Note the ruler in sub-figure B, which shows the size of the articulated hand skeleton. **A**, Articulated hand as originally found in matrix, from Gilmore (1914, fig. 40). **B**, Articulated specimen in the sandbox used for posing. **C**, Proximal view of articulated metacarpus. **D–M**, Oblique views of articulated hand.

In the first four digits of the right hand, the ROM of the proximal phalanx occurs entirely within the field of hyperextension (Fig. 1A, E–G), and the phalanx cannot be flexed any further toward the palm without losing tight articulation with the metacarpal. The phalangeal articular surface of metacarpal I causes the proximal phalanx to twist around its proximodistal axis as it moves (Fig. 1C), so that the surface of the ungual that faces digit II is angled somewhat toward the ground when at maximum extension and is more closely aligned with the long axis of the metacarpal when at maximum flexion (Fig. 1D). The ungual of digit I has very little ROM. It can move through an arc of only 32° (of two-dimensional osteological ROM in the plane of flexion and extension) without losing tight articulation with the proximal phalanx (Fig. 1B). Thus, the ungual, which is not strongly curved but is nearly straight, is nearly in line with metacarpal I when the thumb is fully flexed, instead of being able to curl more toward the palm (Figs 1A and 5).

In the left hand of AMNH FARB 823, ROM in digits I, III and IV cannot be determined. This is because metacarpal I and phalanx I-2 (ungual) are missing, metacarpal III does not fit well with its proximal phalanx, and metacarpal IV is distally eroded. For the proximal phalanx of digit II, I found the two-dimensional osteological ROM, in the plane of flexion and extension to be 47°, all within the field of hyperextension (Fig. 1I), which is similar to the ROM of the homologous phalanx from the right hand. The left hand includes a vestigial phalanx that is reduced to an ovoid nub. It fits with the distal end of phalanx II-1 (Fig. 1H) and not with any other phalanx, which indicates that it is phalanx II-2. It is immobile, as determined by a loss of tight articulation with the proximal phalanx when moved even slightly in any direction.

In the left hand of AMNH FARB 823, the proximal phalanx of digit V is tiny in comparison to its metacarpal. It fits over only one condyle of the metacarpal, leaving the other condyle exposed. It is difficult to determine whether it articulated with the medial

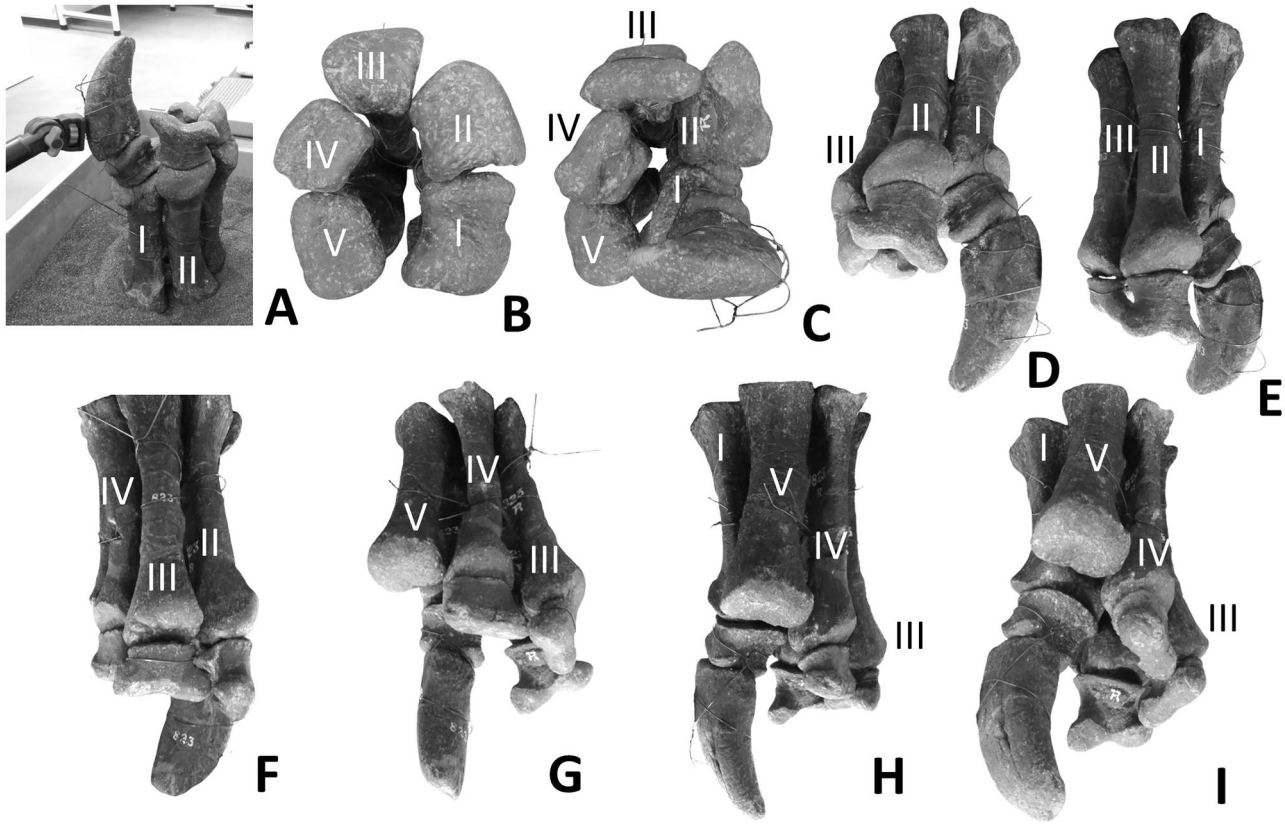

Fig. 5. Articulated right hand skeleton of *Camarasaurus* sp., AMNH FARB 823, posed in full flexion, without phalanges II-2 and V-1 (which are missing from this hand). The sub-figures are reproduced at slightly different scales. Note the ruler in Fig. 3A, which shows the size of the articulated hand skeleton. **A**, Articulated specimen in the sandbox used for posing. **B**, Distal view of articulated metacarpus. **C**, Distal view of articulated hand. **D–I**, Oblique views of articulated hand.

Table 1. Range of motion for each manual phalanx of *Camarasaurus* sp. (AMNH FARB 823) and *Stegosaurus sulcatus* (USNM 4937).

Taxon	Phalanx	Range of motion
Camarasaurus sp.	Right I-1	35°
Camarasaurus sp.	Right I-2	32°
Camarasaurus sp.	Right II-1	53°
Camarasaurus sp.	Right II-2	PM
Camarasaurus sp.	Right III-1	32°
Camarasaurus sp.	Right III-2	PM
Camarasaurus sp.	Right IV-1	11°
Camarasaurus sp.	Right IV-2	PM
Camarasaurus sp.	Right V-1	PM
Camarasaurus sp.	Left I-1	MM
Camarasaurus sp.	Left I-2	PM
Camarasaurus sp.	Left II-1	47°
Camarasaurus sp.	Left II-2	Imm
Camarasaurus sp.	Left III-1	Ind
Camarasaurus sp.	Left III-2	PM
Camarasaurus sp.	Left IV-1	Ind
Camarasaurus sp.	Left IV-2	PM
Camarasaurus sp.	Left V-1	92°
Stegosaurus sulcatus	Right I-1	Imm
S. sulcatus	Right I-2	nearly Imm
S. sulcatus	Right II-1	27°
S. sulcatus	Right III-1	Imm
S. sulcatus	Right IV-1	Imm

Abbreviations: PM, phalanx missing; MM, metacarpal missing; Ind, indeterminate; Imm, immobile.

condyle or the lateral condyle in the living animal, because it fits well with either condyle. The same is the case in finger V of AMNH FARB 965, AMNH FARB 712, and AMNH FARB 332. I arbitrarily used the lateral condyle to measure the two-dimensional osteological ROM, in the plane of flexion and extension, in the proximal phalanx of digit V in AMNH FARB 823. Its ROM is 92°, with 54% (50°) of that ROM in the field of hyperextension and with a great degree of flexion (42°) toward the palm (Fig. 1J; Table 1). Despite its large degree of flexion, digit V cannot collide with or obstruct the movement of any other digit during finger flexion, because the ROM of each other finger is entirely within the field of hyperextension.

Stegosaurus sulcatus

There is very little range of motion in the hand of *Stegosaurus*. The distal end of each metacarpal is saddle-shaped: rounded and convex in the flexor-extensor plane, and concave in the adductor-abductor

plane. In fingers I, III and IV, the proximal phalanx is immobile. It fits only on a specific spot on the metacarpal (Fig. 2A, C, E), and if it is moved even slightly, the transversely concave shape of the metacarpal's distal surface introduces a gap between the metacarpal and the middle of the phalanx's articular surface, so that the phalanx is no longer fully articulated with the metacarpal. The proximal phalanx of digit II is mobile but can move only through a very small arc of 27° (of two-dimensional osteological ROM in the plane of flexion and extension) without losing tight articulation with the metacarpal (Fig. 2B; Table 1). The proximal end of the ungual phalanx of finger I has a small articular surface for the proximal phalanx, allowing a little wobble but not enough ROM to be measurable. The proximal phalanges of fingers III and IV have no ROM (Table 1). Each loses articulation with its metacarpal, due to the gap that the metacarpal's transversely concave distal surface introduces, if the phalanx is moved even slightly. In fingers III and IV, the metacarpal's articular surface for the phalanx is distal, so the phalanx is between the metacarpal and the ground when the metacarpus is vertical (Fig. 2C, E). In these two fingers, the proximal phalanx also fits snugly with a surface immediately proximal to the articular surface, on the extensor surface of the metacarpal (Fig. 2D, F). However, this surface of the metacarpal bears the longitudinal grooves characteristic of the non-articular surface immediately proximal to the articular surface on the metacarpals of other dinosaur species, which indicates that this surface of the metacarpal is a non-articular surface, despite the fact that it fits well with the proximal articular surface of the phalanx. In finger IV, the distal end of the metacarpal is divided into two facets, one on the pollucal side and one on the side toward digit II. The former facet is slanted so that most of it does not extend as far distally as the latter facet. The proximal phalanx of finger IV is situated between this slanted surface and the ground (Fig. 4I, J).

Discussion

Tschopp *et al.* (2015) described a specimen of *Camarasaurus* in which the hand skeletons were preserved in articulation. That specimen confirms such findings of this study as the slanted orientation of the thumb ungual and the position of the vestigial phalanx II-2. The slanted orientation of the thumb ungual also occurs in other sauropods, as Elmer Riggs concluded from the shapes of the bony articular surfaces over a century ago (Osborn 1904). The proximal phalanges of the *Camarasaurus* specimen described by Tschopp *et al.* (2015) were positioned distally to their respective metacarpals, in approximately the position found here for maximum flexion of fingers I–IV, thus supporting this study's finding that these phalanges could achieve this position. The proximal phalanges were located distally to the metacarpals in the juvenile *Camarasaurus* specimen described by Gilmore (1925), but that specimen is less informative in this regard, because its hand skeletons were articulated to a lesser degree.

The positioning of the immobile proximal phalanx of finger III and that of finger IV in *Stegosaurus*, so that the phalanx sits between the metacarpal and the ground, is unexpected in an animal that keeps its metacarpus vertical. This would at first seem to introduce instability, because the transversely broad metacarpal would have been balanced upon a transversely narrow phalanx. However, this finding of the present study is consistent with the *in situ* configuration of the specimen's other hand, in which the metacarpals were found arranged in an arc and the proximal phalanges of fingers III and IV were positioned distally to their respective metacarpals (Gilmore 1914, fig. 40). Furthermore, the manus prints of *Deltapodus* Whyte & Romano, 2001—an ichnogenus that is thought to represent stegosaur tracks—lack clear imprints of fingers II–IV extending from the metacarpal arc (Whyte & Romano 2001, fig. 3; Guillaume *et al.* 2022, fig. 5; Castanera *et al.* 2024, figs 5, 8). This is consistent with the positioning of the phalanx on the distal surface instead of the extensor surface. This suggests that instability in the hand was prevented by some part of the animal that did not fossilize, such as a thick pad or pads of tough, possibly fibrous soft tissue in the hand, which provided support to the metacarpals' tips.

This study's examination of only one *Stegosaurus* hand is, admittedly, a limitation. Unfortunately, only a few other stegosaur specimens with both metacarpals and manual phalanges are known. These include a specimen of *Miragaia longicollum* Mateus, Maidment & Christiansen, 2009 (Mateus *et al.* 2009) and a juvenile *Stegosaurus* sp. (Galton 1982). It would be interesting to compare their manual ROM with that of USNM 4937 in a future study. Hennig (1925) described a specimen of *Kentrosaurus aethiopicus* Hennig, 1915 with metacarpals and possible manual phalanges, but he noted that the latter resembled the pedal phalanges, and he was unable to determine whether the phalanges were indeed manual.

The metacarpals of basal sauropodomorphs and basal ornithischians were arranged in a shallow arc in proximal view, not in a tubular or semi-tubular configuration (Santa Luca 1980, Bonnan 2003). The evolutionary lineages leading to *Camarasaurus* and *Stegosaurus* therefore gained their tubular metacarpal configurations independently. But in each lineage, the predicament that the new metacarpal configuration would otherwise have caused (crowding and impeded movement of fingers during flexion) was prevented in the same way: reduction of the distal portion of each finger, and limitation of finger flexion. Sauropods and stegosaurs thus provide an example of convergent evolution not only in the configuration of the metacarpus but also in the morphology and ROM of the fingers.

This shared method of preventing the crowding of fingers and their obstruction of each other's motion resulted in another shared functional trait of the forelimb. The fingers of *Camarasaurus* and *Stegosaurus* lacked the ability to contribute to propulsion *via* strong flexion toward the caudal end of the animal, because the fingers of *Camarasaurus* flexed toward each other, and only one of the fingers of *Stegosaurus* could flex at all. Propulsion by means of the forelimb must therefore have been accomplished at the more proximal joints: shoulder, elbow, and wrist. Trackway evidence supports this conclusion. Tracks of birds and non-avian theropod dinosaurs in sufficiently soft mud are deeper at the toe tips than at the metatarsal pad, demonstrating that the toes exerted pressure that was used in forward propulsion (Gatesy *et al.* 1999). In contrast, sauropod manus tracks are not deeper at the fingertips than more proximally. This, in addition to the lack of any indication of dragging of the thumb claw or the other fingers, indicates that the manus was both planted and lifted vertically, which means that propulsion must have been accomplished by forelimb segments proximal to the hand (Milàn *et al.* 2005, Farlow *et al.* 1989, fig. 42.6; Pittman & Gillette 1989, figs 34.15, 34.16; Santos *et al.* 1994, fig. 7, Salisbury *et al.* 2016, figs 26, 32, 35). The same is the case for stegosaur manus tracks (Salisbury *et al.* 2016, figs 48, 50; Guillaume *et al.* 2022, fig. 5; Castanera *et al.* 2024, fig. 5).

Some previous authors have noted that sauropod manus tracks often lack an impression of the thumb claw and have hypothesized that the explanation for this is that sauropods held the thumb in strong hyperextension (Thulborn 1989) or that sauropods walked on their knuckles with the thumb and other fingers in strong flexion toward the palm (de Beaumont & Demathieu 1980). The results of this study show that the hand of *Camarasaurus* was not capable of either of these poses. It could not hyperextend its thumb sufficiently to avoid making a claw print, and none of its fingers were capable of sufficiently strong flexion to enable knuckle-walking (Fig. 1). A plausible explanation for the lack of thumb claw impressions in the sauropod manus tracks in question is that they were made by members of the Titanosauria, a sauropod clade in which the phalanges were lost (Apesteguía 2005). Sauropod manus tracks in which a thumb claw impression is present (e.g., Santos *et al.* 1994, Milàn *et al.* 2005, Salisbury *et al.* 2016, 53) were apparently made by non-titanosaurian sauropods.

Conclusions

ROM in the fingers of *Camarasaurus* and *Stegosaurs* differs strongly from that of the other quadrupedal dinosaurs for which manual ROM has been investigated: the ornithopod dinosaur *Uteodon* McDonald, 2011 (Carpenter & Wilson 2008) and the ceratopsian dinosaur *Leptoceratops* Brown, 1914 (Senter 2007). In *Camarasaurus*, ROM in fingers I–IV is limited to the field of hyperextension. In *Stegosaurus*, such is the case for finger II, and the phalanges of the other fingers are immobile. In contrast, only the thumb has a small ROM in the ornithopod *Uteodon*. Its fingers II–V can swing through a broad arc, both in the field of hyperextension and in the field of flexion toward the palm (Carpenter & Wilson 2008). The same is the case in fingers I–III of *Leptoceratops* (Senter 2007). Finger ROM is therefore much more limited in *Camarasaurus* and *Stegosaurus* than it is in these two other quadrupedal dinosaurs.

This difference between *Camarasaurus* and *Stegosaurus* on the one hand, versus *Uteodon* and *Leptoceratops* on the other hand, is functionally related to the arrangement of the metacarpals. The articulated metacarpals form a tube in *Camarasaurus* and a semi-tube in *Stegosaurus*, whereas in proximal view they are arranged in a shallow arc in *Uteodon* (Carpenter & Wilson 2008, fig. 46B) and *Leptoceratops* (Senter 2007, fig. 6f). A tubular or semi-tubular arrangement of the metacarpals aims the fingers toward each other during flexion, which would cause them to hit each other and thereby obstruct each other's movement if they had the high degree of flexion that is present in the fingers of *Uteodon* and *Leptoceratops*. The limited ROM in the fingers of *Camarasaurus* and *Stegosaurus* prevents this potential

predicament by preventing the fingers from moving far enough toward each other to crowd or obstruct each other.

Acknowledgements

Carl Mehling (AMHH) and Matthew Miller (USNM) provided access to specimens. Heinrich Mallison and an anonymous reviewer provided useful input that improved this manuscript.

Disclosure statement

The author states that there are no competing interests to declare.

Funding statement

This research was undertaken without funding.

References

Apesteguía, S., 2005. Evolution of the titanosaur metacarpus. In *Thunder-Lizards: The Sauropodomorph Dinosaurs*. Tidwell, V. & Carpenter, K., eds. Indiana University Press, Bloomington, 321–345.

Arnold, P., Fischer, M.S. & Nyakatura, J.A., 2014. Soft tissue influence on *ex vivo* mobility in the hip of *Iguana*: comparison with *in vivo* movement and its bearing on joint motion of fossil sprawling tetrapods. *Journal of Anatomy 225*, 31–41.

Baier, D.B. & Gatesy, S.M., 2013. Three-dimensional skeletal kinematics of the shoulder girdle and forelimb in walking *Alligator*. *Journal of Anatomy 223*, 462–473.

Bonnan, M.F., 2003. The evolution of manus shape in sauropod dinosaurs: implications for functional morphology, forelimb orientation, and phylogeny. *Journal of Vertebrate Paleontology 23*, 595–613.

Carpenter, K., 2002. Forelimb biomechanics of nonavian theropod dinosaurs in predation. *Senckenbergiana Lethaea 82*, 59–75.

Carpenter, K., Bartlett, J., Bird, J. & Barrick, R., 2008. Ankylosaurs from the Price River quarries, Cedar Mountain Formation (Lower Cretaceous), east-central Utah. *Journal of Vertebrate Paleontology 28*, 1089–1101.

Carpenter, K. & Wilson, Y., 2008. A new species of Camptosaurus (Ornithopoda: Dinosauria) from the Morrison Formation (Upper Jurassic) of Dinosaur National Monument, Utah, and a biomechanical analysis of its forelimb. *Annals of Carnegie Museum 76*, 227–263.

Castanera, D., Mampel, L. & Cobos, A., 2024. The complexity of tracking stegosaurs and their gregarious behavior. *Scientific Reports 14*, 14833.

Coombs, W.P., JR., 1978. Theoretical aspects of cursorial adaptations in dinosaurs. *The Quarterly Review of Biology 53*, 393–418.

De Beaumont, G. & Dematheiu, G., 1980. Remarques sur les extremités antérieurs des Sauropodes (Reptiles, Saurischiens). *Comptes Rendus des Séances, Société d'Histoire Naturelle de Genève (Nouvelle Série) 15*, 191–198.

Dempsey, M., Maidment, S.C.R., Hedrick, B.P. & Bates, K.T., 2023. Convergent evolution of quadrupedality in ornithischian dinosaurs was achieved through disparate forelimb muscle mechanics. *Proceedings of the Royal Society B* 290(20222425), 1–12.

Demuth, O.E., Rayfield, E.J. & Hutchinson, J.R., 2020. 3D hindlimb joint mobility of the stem-archosaur *Euparkeria capensis* with implications for postural evolution within Archosauria. *Scientific Reports 10*, 15357.

Demuth, O.E., Herbst, E., Polet, D.T., Wiseman, A.L.A. & Hutchinson, J.R., 2023. Modern three-dimensional digital methods for studying locomotor biomechanics in tetrapods. *Journal of Experimental Biology 226*, 1–12.

Farlow, J.O., Pittman, J.G. & Hawthorne, J.M., 1989. *Brontopodus birdi*, Lower Cretaceous sauropod footprints from the U.S. Gulf Coastal Plain. In *Dinosaur Tracks and Traces*. Gillette, D.D. & Lockley, M.G., eds. Cambridge University Press, Cambridge, 371–394.

Galton, P.M., 1971. Manus movements of the coelurosaurian dinosaur *Syntarsus* and opposability of the theropod hallux. *Arnoldia 15*, 1–8.

Galton, P.M., 1982. Juveniles of the stegosaurian dinosaur *Stegosaurus* from the Upper Jurassic of North America. *Journal of Vertebrate Paleontology 2*, 47–62.

Galton, P.M. & Upchurch, P., 2004. Stegosauria. In *The Dinosauria*, 2nd ed., Weishampel, D.B., Dodson, P. & Osmólska, H., eds. University of California Press, Berkeley, 343–362.

Gatesy, S.M., Middleton, K.M., Jenkins, F.A., JR. & Shubin, N.H., 1999. Three-dimensional preservation of foot movements in Triassic theropod dinosaurs. *Nature 399*, 141–144.

Gilmore, C.W., 1914. Osteology of the armored Dinosauria in the United States National Museum, with special reference to the genus *Stegosaurus*. *United States National Museum Bulletin 89*, 1–143.

Gilmore, C.W., 1925. A nearly complete articulated skeleton of *Camarasaurus*, a saurischian dinosaur from the Dinosaur National Monument, Utah. *Memoirs of the Carnegie Museum 10*, 347–384.

Gishlick, A.D., 2001. The function of the manus and forelimb of *Deinonychus antirrhopus* and its importance for the origin of avian flight. In *New Perspectives on the Origin and Early Evolution of Birds*, Gauthier, J. & Gall, L.F., eds. Yale Peabody Museum, New Haven, 301–318.

Guillaume, A.R.D., Costa, F. & Mateus, O., 2022. Stegosaur tracks from the Upper Jurassic of Portugal: new occurrences and perspectives. *Ciências da Terra - Earth Sciences Journal 20*, 37–60.

Hatcher, J.B., 1902. Structure of the fore limb and manus of *Brontosaurus*. *Annals of the Carnegie Museum 1*, 356–376.

Hennig, E., 1925. *Kentrurosaurus aethiopicus*, die Stegosaurier-Funde vom Tendaguru, Deutsch-Ostafrika. *Palaeontographica Supplement 7*, 101–254.

Holliday, C.M., Ridgely, R.C., Sedlmayr, J.C. & Witmer, L.M., 2010. Cartilaginous epiphyses in extant archosaurs and their implications for reconstructing limb function in dinosaurs. *PloS One 5*, e13120.

Hutson, J.D. & Hutson, K.N., 2012. A test of the validity of range of motion studies of fossil archosaur elbow mobility using repeated-measures analysis and the extant phylogenetic bracket. *The Journal of Experimental Biology 215*, 2030–2038.

Hutson, J.D. & Hutson, K.N., 2013. Using the American alligator and a repeated-measures design to place constraints on *in vivo* shoulder joint range of motion in dinosaurs and other fossil archosaurs. *The Journal of Experimental Biology 216*, 275–284.

Hutson, J.D. & Hutson, K.N., 2015. Inferring the prevalence and function of finger hyperextension in Archosauria from finger-joint range of motion in the American alligator. *Journal of Zoology 296*, 189–199.

Janensch, W., 1961. Die Gliedmaszen und Gliedmaszengürtel der Sauropoden der Tendaguru-Schichten. *Paläontographica Supplement 7*, 177–235.

Kambic, R.E., Roberts, T.J. & Gatesy, S.M., 2014. Long-axis rotation: a missing degree of freedom in avian bipedal locomotion. *The Journal of Experimental Biology 217*, 2770–2782.

Kambic, R.E., Roberts, T.J. & Gatesy, S.M., 2017. 3-D range of motion envelopes reveal interacting degrees of freedom in avian hind limb joints. *Journal of Anatomy 231*, 906–920.

Kobayashi, K. & Barsbold, R., 2005. Anatomy of *Harpymimus okaldnikovi* Barsbold and Perle 1984 (Dinosauria; Theropoda) of Mongolia. In *The Carnivorous Dinosaurs*., Carpenter, K., ed. Indiana University Press, Bloomington, 97–126.

Kobayashi, K., Zelenitsky, D.K., Fiorillo, A.R. & Chinzorig, T., 2025. Didactyl therizinosaur with a preserved keratinous claw from the Late Cretaceous of Mongolia. *iScience 28*, 113214.

Mallison, H., 2010. The digital *Plateosaurus* II: an assessment of the range of motion of the limbs and vertebral column and of previous reconstructions using a digital skeletal mount. *Acta Palaeontologica Polonica 55*, 433–458.

Manafzadeh, A.R. & Gatesy, S.M., 2021. Paleobiological reconstructions of articular function require all six degrees of freedom. *Journal of Anatomy 239*, 1516–1524.

Manafzadeh, A.R. & Padian, K., 2018. ROM mapping of ligamentous constraints on avian hip mobility: implications for extinct ornithodirans. *Proceedings of the Royal Society B* 285(20180727), 1–9.

Manafzadeh, A.R., Gatesy, S.M. & Bhullar, B.-A.S., 2024. Articular surface interactions distinguish dinosaurian locomotor joint poses. *Nature Communications 15*, 854.

Mateus, O., Maidment, S.C.R. & Christiansen, N.A., 2009. A new long-necked "sauropod-mimic" stegosaur and the evolution of the plated dinosaurs. *Proceedings of the Royal Society B* 276, 1815–1821.

Microsoft Corporatioon 2025. *Microsoft Paint Version 11.2507.371.0*. Redmond, Washington: Microsoft Corporation.

Microsoft Corporatioon 2026. *Microsoft PowerPoint Version 2605*. Redmond, Washington: Microsoft Corporation.

Milàn, J., Christiansen, P. & Mateus, O., 2005. A three-dimensionally preserved sauropod manus impression from the Upper Jurassic of Portugal: implications for sauropod manus shape and locomotor mechanics. *Kaupia, Darmstädter Beiträge zur Naturgeschichte 14*, 47–52.

Nicholls, E.L. & Russell, A.P., 1985. Structure and function of the pectoral girdle and forelimb of *Struthiomimus altus* (Theropoda: Ornithomimidae). *Palaeontology 28*, 643–677.

Osborn, H.F., 1904. Manus, sacrum, and caudals of Sauropoda. *Bulletin of the American Museum of Natural History 20*, 181–190.

Osmólska, H. & Roniewicz, E., 1969. Deinocheiridae, a new family of theropod dinosaurs. *Palaeontologia Polonica 27*, 5–19.

Pierce, S.E., Clack, J.A. & Hutchinson, J.R., 2012. Three-dimensional limb joint mobility in the early tetrapod *Ichthyostega*. *Nature 486*, 523–526.

Pittman, J.G. & Gillette, D.D., 1989. The Briar Site: a new sauropod dinosaur tracksite in Lower Cretaceous beds of Arkansas, USA. In *Dinosaur Tracks and Traces*. Gillette, D.D. & Lockley, M.G., eds. Cambridge University Press, Cambridge, 313–332.

Reiss, S. & Mallison, H., 2014. Motion range of the manus of *Plateosaurus engelhardti* von Meyer, 1837. *Palaeontologia Electronica 17*, 1–19.

Richards, H.L., Bishop, P.J., Hocking, D.P., Adams, J.W. & Evans, A.R., 2021. Low elbow mobility indicates unique forelimb posture and function in a giant extinct marsupial. *Journal of Anatomy 238*, 1425–1441.

Salisbury, S.W., Romilio, A., Herne, M.C., Tucker, R.T. & Nair, J.P., 2016. The dinosaurian ichnofauna of the Lower Cretaceous (Valanginian–Barremian) Broome Sandstone of the Walmadany area (James Price Point), Dampier Peninsula, Western Australia. *Journal of Vertebrate Paleontology 36*, 1–152.

Santa Luca, A.P., 1980. The postcranial skeleton of *Heterodontosaurus tucki* (Reptilia, Ornithischia) from the Stormberg of South Africa. *Annals of the South African Museum 79*, 159–211.

Santos, V.F., Lockley, M.G., Meyer, C.A., Carvalho, J., Galopim, D.E., Carvalho, A.M. & Moratalla, J.J., 1994. A new sauropod tracksite from the Middle Jurassic of Portugal. *Gaia 10*, 5–13.

Senter, P., 2005. Function in the stunted forelimbs of *Mononykus olecranus* (Theropoda), a dinosaurian anteater. *Paleobiology 31*, 373–381.

Senter, P., 2006a. Comparison of forelimb function between *Deinonychus* and *Bambiraptor* (Theropoda: Dromaeosauridae). *Journal of Vertebrate Paleontology 26*, 897–906.

Senter, P., 2006b. Forelimb function in *Ornitholestes hermanni* Osborn (Dinosauria, Theropoda). *Palaeontology 49*, 1029–1034.

Senter, P., 2007. Analysis of forelimb function in basal ceratopsians. *Journal of Zoology 273*, 305–314.

Senter, P., 2009. Pedal function in deinonychosaurs (Dinosauria: Theropoda): a comparative study. *Bulletin of Gunma Museum of Natural History 13*, 1–14.

Senter, P., 2010. Evidence for a sauropod-like metacarpal configuration in stegosaurian dinosaurs. *Acta Palaeontologica Polonica 55*, 427–432.

Senter, P., 2011. Evidence for a sauropod-like metacarpal configuration in ankylosaurian dinosaurs. *Acta Palaeontologica Polonica 56*, 221–224.

Senter, P. & Parrish, J.M., 2005. Functional analysis of the hands of the theropod dinosaur *Chirostenotes pergracilis*: evidence for an unusual paleoecological role. *PaleoBios 25*, 9–19.

Senter, P. & Parrish, J.M., 2006. Forelimb function in the theropod dinosaur *Carnotaurus sastrei*, and its behavioral implications. *PaleoBios 26*, 7–17.

Senter, P. & Robins, J.H., 2005. Range of motion in the forelimb of the theropod dinosaur *Acrocanthosaurus atokensis*, and implications for predatory behaviour. *Journal of Zoology 266*, 307–318.

Senter, P.J. & Sullivan, C., 2019. Forelimbs of the theropod dinosaur *Dilophosaurus wetherilli*: range of motion, influence of paleopathology and soft tissues, and description of a distal carpal bone. *Palaeontologia Electronica 22*, 1–19.

Sereno, P.C., 1994. Pectoral girdle and forelimb of the basal theropod *Herrerasaurus ischigualastensis*. *Journal of Vertebrate Paleontology 13*, 425–450.

Thompson, S. & Holmes, R., 2007. Forelimb stance and step cycle in *Chasmosaurus irvinensis* (Dinosauria: Neoceratopsia). *Palaeontologia Electronica 10*, 1–17.

Thulborn, R.A., 1989. The gaits of dinosaurs. In *Dinosaur Tracks and Traces*. Gillette, D.D. & Lockley, M.G., eds. Cambridge University Press, Cambridge, 39–50.

Tschopp, E., Wings, O., Frauenfelder, T. & Brinkmann, W., 2015. Articulated bone sets of manus and pedes of *Camarasaurus* (Sauropoda, Dinosauria). *Palaeontologia Electronica 18*, 1–65.

Upchurch, P., Barrett, P.M. & Dodson, P., 2004. Sauropoda. In *The Dinosauria*., 2nd ed., Weishampel, D.B., Dodson, P. & Osmólska, H., eds. University of California Press, Berkeley, 259–322.

Welles, S.P., 1984. *Dilophosaurus wetherilli* (Dinosauria, Theropoda). Osteology and comparisons. *Palaeontographica Abteilung A 185*, 85–180.

White, M.A., Bell, P.R., Cook, A.G., Barnes, D.G., Tischler, T.R., Bassam, B.J. & Elliott, D.A., 2015. Forearm range of motion in *Australovenator wintonensis* (Theropoda, Megaraptoridae). *PloS One 10*, e0137709.

White, M.A., Cook, A.G., Klinkhamer, A.J. & Elliott, D.A., 2016. The pes of *Australovenator wintonensis* (Theropoda: Megaraptoridae): analysis of the pedal range of motion and biological restoration. *PeerJ. 4*, e2312.

Whyte, M.A. & Romano, M., 2001. Probable stegosaurian dinosaur tracks from the Saltwick Formation (Middle Jurassic) of Yorkshire, England. *Proceedings of the Geologists' Association* 112, 45–54.

Wiseman, A.L.A., Demuth, O.E., Pomeroy, E. & DE Groote, I., 2022. Reconstructing articular cartilage in the *Australopithecus afarensis* hip joint and the need for modeling six degrees of freedom. *Integrative Organismal Biology 4*, 1–20.